*J Neuropathol Exp Neurol*
Vol. 77, No. 10, October 2018, pp. 877–882
doi: 10.1093/jnen/nly064

BRIEF REPORT

# Neuropathology of a Case With Fatal CAR T-Cell-Associated Cerebral Edema

Matthew Torre, MD, Isaac H. Solomon, MD, PhD, Claire L. Sutherland, PhD, Sarah Nikiforow, MD, PhD, Daniel J. DeAngelo, MD, PhD, Richard M. Stone, MD, Henrikas Vaitkevicius, MD, Ilene A. Galinsky, NP, Robert F. Padera, MD, PhD, Nikolaus Trede, MD, PhD, and Sandro Santagata, MD, PhD

**Abstract**

Chimeric antigen receptor (CAR) T cells are a new and powerful class of cancer immunotherapeutics that have shown potential for the treatment of hematopoietic malignancies. The tremendous promise of this approach is tempered by safety concerns, including potentially fatal neurotoxicity, sometimes but not universally associated with cytokine release syndrome. We describe the postmortem examination of a brain from a 21-year-old patient with relapsed pre-B cell acute lymphoblastic leukemia (ALL) who died from fulminant cerebral edema following CAR T-cell infusion. We found a range of changes that included activation of microglia, expansion of perivascular spaces by proteinaceous exudate, and clasmatodendrosis—a beading of glial fibrillary acidic protein consistent with astrocyte injury. Notably, within the brain parenchyma, we identified only infrequent T cells and did not identify ALL cells or CAR T cells. The overall findings are nonspecific but raise the possibility of astrocyte and blood-brain barrier dysfunction as a potential etiology of fatal CAR T-cell neurotoxicity in this patient.

**Key Words:** Blood-brain barrier (BBB), Chimeric antigen receptor (CAR) T cells, Cerebral edema, Chimeric antigen receptor T cells, Cytokine release syndrome (CRS), Neurotoxicity.

From the Department of Pathology, Brigham and Women's Hospital, Harvard Medical School, Boston, Massachusetts (MT, IHS, RFP, SS); JUNO Therapeutics, Seattle, Washington (CLS, NT); Department of Medical Oncology, Dana-Farber Cancer Institute, Harvard Medical School, Boston, Massachusetts (SN, DJD, RMS, IAG); Department of Neurology, Brigham and Women's Hospital, Harvard Medical School, Boston, Massachusetts (HV); Department of Oncologic Pathology, Dana-Farber Cancer Institute, Boston, Massachusetts (SS); and Lab for Systems Pharmacology, Harvard Medical School, Boston, Massachusetts (SS).

Send correspondence to: Sandro Santagata, MD, PhD, Department of Pathology, Brigham and Women's Hospital, 75 Francis Street, Boston, MA 02115; E-mail: ssantagata@bics.bwh.harvard.edu

There are no sources of funding to disclose.

JUNO Therapeutics sponsored the ROCKET phase 2 clinical trial of CAR T-cell therapy JCAR015 for the treatment of patients with acute lymphocytic leukemia. Juno therapeutics did not fund the work presented in this manuscript. Claire L. Sutherland is the director of translational medicine at JUNO. Nikolaus Trede is the senior medical director at JUNO. Richard M. Stone and Daniel J. DeAngelo were ad hoc consultants to JUNO. For the remaining authors, no conflicts of interest were declared.

Supplementary Data can be found at academic.oup.com/jnen.

## INTRODUCTION

Chimeric antigen receptor (CAR) T cells are T lymphocytes engineered to express recombinant receptors comprising a tumor recognition region, a T-cell receptor intracellular signaling domain, and typically an intervening costimulatory domain. Anti-CD19 CAR T cells have produced significant and durable therapeutic responses in patients with relapsed/refractory B-ALL and other hematopoietic malignancies (1–4). Significant side effects are often encountered, including systemic inflammatory cytokine release syndrome (CRS) and mild to severe neurotoxicity manifested by varying degrees of cognitive dysfunction, focal neurologic deficits, and sometimes seizures. CAR T-cell-associated neurotoxicity can occur with or without concomitant CRS (5).

Fatal cerebral edema is the most extreme example of neurotoxicity encountered during CAR T-cell therapy. Although the precise mechanism of CAR T-cell therapy-associated cerebral edema is unclear, cytokine-mediated endothelial activation, aberrant angiopoietin 1 (ANG1) and angiopoietin 2 (ANG2) signaling, and increased blood-brain barrier (BBB) permeability could play a role (5). Risk factors for developing neurotoxicity include disease burden, higher grades of CRS, and overexpression of cytokines such as IFNγ, TNFα, IL-1, and IL-6 (6, 7). Anti-IL-6 receptor therapy with tocilizumab can ameliorate CRS but generally has no therapeutic effect on neurotoxicity and may actually exacerbate the presentation (1, 6).

Recently, an anti-CD19 CAR T-cell therapy clinical trial (NCT02535364) was terminated after several deaths from fulminant cerebral edema (8). Here, we report the postmortem examination from one of these patients.

## CASE REPORT

The patient was a 21-year-old man who developed B-cell ALL in 2005 at age 11 and was treated with a chemotherapy regimen similar to Children's Oncology Group protocol AALL0232 (9) for a total of 3 years. The disease recurred in 2012, and a second complete remission was achieved with therapy following COG AALL0433 (10). In April 2016, the patient experienced a second relapse and was enrolled in JUNO Therapeutics' clinical trial of anti-CD19 CAR T cells

(ROCKET). Bone marrow examination at the time of study enrollment showed CD45, HLA-DR, CD19, CD20, CD10-positive B cells involving >95% of the intertrabecular space. A next-generation sequencing assay of genes recurrently mutated in hematologic malignancies was performed on peripheral blood, revealing an NRAS G12S mutation in 18% of reads. Cytogenetics performed on leukemia cells from the bone marrow showed a complex karyotype with multiple trisomies. The patient underwent apheresis of T cells and then prior to CAR T-cell manufacturing was administered FLAG chemotherapy consisting of fludarabine, cytosine arabinoside, and G-CSF. This treatment was complicated by neutropenic fevers and presumptive hepatosplenic candidiasis that was treated and controlled with broad spectrum antibacterial agents and micafungin.

In June 2016, approximately 1 month after the initiation of FLAG, the patient remained clinically stable but still had high disease burden, with a bone marrow aspirate containing 65% blasts. At that point, the patient received lymphodepleting therapy consisting of 1 intravenous (IV) dose of cyclophosphamide (60 mg/kg) followed by 3 daily IV doses of fludarabine (25 mg/m$^2$). The patient had an extensive neurological examination which was unremarkable, including normal cognition and mini-mental state exam. He did not report peripheral neuropathy. Four days later, he received a CAR T-cell infusion of $1.2\times10^6$ CD3+ CAR+ cells/kg. The following day, he developed low-grade fevers and tachycardia. The patient was treated with IV fluids, 8 mg/kg tocilizumab, and dexamethasone 10 mg IV for Grade 2 CRS on the second day following infusion (6). The patient demonstrated no neurologic changes until the late afternoon of the fourth day postinfusion, when he had subtle word-finding difficulties and a concomitant fever of 103°F.

At 6:30 pm on the fourth day after infusion, the patient rapidly became lethargic (CTCAE Grade 1 neurotoxicity), for which he was given 20 mg of IV dexamethasone and 1 g of IV levetiracetam. By 7:45 pm, he was unresponsive (CTCAE Grade 3 neurotoxicity), eventually undergoing endotracheal intubation (CTCAE Grade 4 neurotoxicity). A head CT performed at 8:30 pm showed no evidence of an acute intracranial abnormality, but a head CT performed 4 hours later for fixed and dilated pupils showed diffuse cerebral edema (Fig. 1A). Serum ferritin (14,710 µg/L, baseline 2500–3000 µg/L) and D-dimers were elevated (>4000 ng/mL, baseline 500–900 ng/mL). CRP remained persistently elevated (>30 mg/L, baseline 5.3 mg/L) following multiple dexamethasone administrations but was lower than the pre-CAR T-cell infusion peak of 168 mg/L. Fibrinogen had risen following CAR T-cell infusion (500–700 mg/dL) but dropped concurrent with the onset of neurotoxicity (403 mg/dL). Creatine was slightly elevated (up to 1.24 mg/dL, baseline 0.50–0.70 mg/dL), and there was a mild transaminitis (ALT up to 90 U/L, baseline 20–40 U/L; AST up to 150 U/L, baseline 20–40 U/L) (Supplementary Data Table S1). Ventriculostomy was attempted but not possible due to complete effacement of the ventricular system. Mannitol, additional dexamethasone, and hyperventilation were administered.

The patient's clinical exam became consistent with brain death, which was confirmed by single-photon emission computerized tomography (SPECT) scan performed on the fifth day postinfusion. Death was pronounced based on brain death criteria and supportive care was discontinued. We performed an autopsy approximately 36 hours after death.

## MATERIALS AND METHODS

We fixed all organs in formalin and examined the histology of non-CNS tissues as well as the hippocampus, amygdala, cerebellum, basal forebrain, striatum, thalamus, brainstem, medulla, pons, midbrain, spinal cord and each lobe of the cerebral cortex. We examined the tissue using light microscopy after routine stains as well as immunohistochemistry (IHC) and immunofluorescence. IHC was performed on 5-µm formalin-fixed, paraffin-embedded (FFPE) sections following routine heat antigen retrieval (10 mM sodium citrate buffer, pH 6.0). The primary antibodies used were CD3 (1:300; Leica, Richmond, IL), CD20 (1:300; DAKO, Carpinteria, CA), LCA (1:500; DAKO), CD68 (1:1000; DAKO), GFAP (1:15 000; DAKO), GLUT1 (1:1500, DAKO), factor VIIIA (1:500; Biogenex, Fremont, CA), ICAM-1 (1:1200; Abcam, Cambridge, MA), and VCAM-1 (1:1000; Abcam). Nuclei were counterstained with Mayer's hematoxylin. Endothelial ICAM-1 and VCAM-1 expression was assessed by visual review of 20 randomly selected blood vessels in each section of the patient's frontal, temporal, and occipital cortex. Additional paraffin sections were used for special stains, including Luxol fast blue with periodic acid-Schiff (LFB-PAS) and Gomori methenamine silver stain (MSS), according to standard protocols. The phosphotungstic acid hematoxylin (PTAH) method was used on paraffin sections to stain for fibrin. Immunofluorescence for fibrin (1:40; DAKO) was performed on frozen tissue sections.

To evaluate for the presence of CAR T cells, we used a custom probe to the chimeric CD19 receptor for chromogenic in situ hybridization (CISH) that was performed as described by the manufacture's protocol (Advanced Cell Diagnostics, Newark, CA). As a control, we used 5-µm FFPE sections of cell pellets generated by spiking JCAR015 CAR T cells into healthy donor peripheral blood mononuclear cells.

We attempted ultrastructural examination of pieces from the occipital cortex and white matter that had been fixed in glutaraldehyde. However, suboptimal tissue preservation precluded high-resolution imaging and assessment of the ultrastructure of the blood-brain barrier. We used sections of cortex from 10 control autopsy cases with postmortem intervals ranging from 26 to 88 hours for the analysis of GFAP, ICAM-1 and VCAM-1 expression and localization by immunohistochemistry and fibrin localization by immunofluorescence.

## RESULTS

Gross examination of the brain showed widespread, severe edema. The weight was markedly increased (1680 g, normal 1250–1400 g), the gyri were flattened, and the sulci (Fig. 1B), ventricles (Fig. 1C) and cerebral aqueduct were substantially compressed. Tonsillar, uncal, and subfalcine herniations, however, were absent. There were neither Duret nor intraparenchymal hemorrhages.

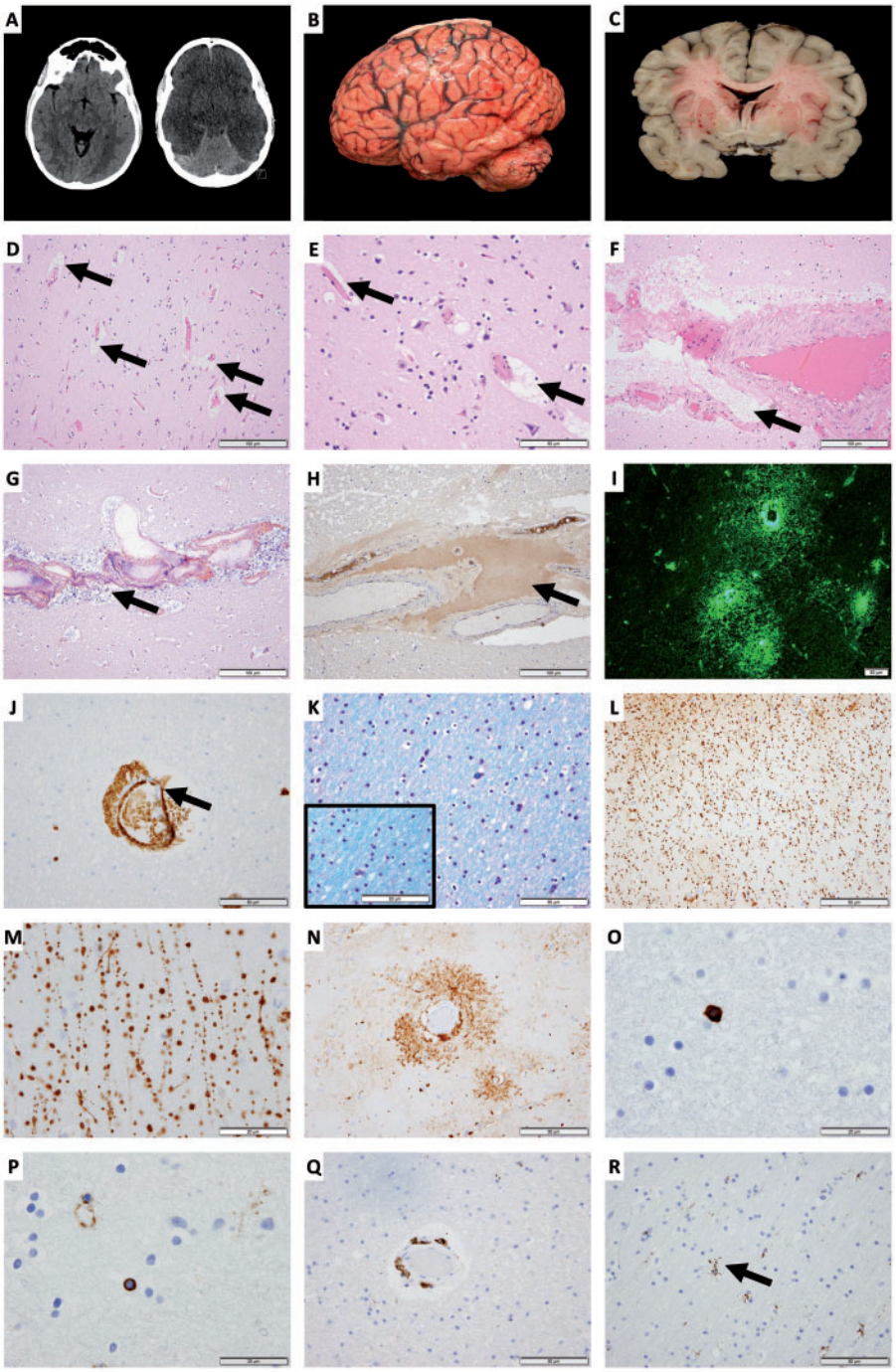


**FIGURE 1. (A)** Head CTs taken 4 hours apart, demonstrating rapid progression from normal (left) to diffuse, severe cerebral edema (right); **(B)** gross photograph of the brain with flattened gyri and tightened sulci; **(C)** coronal section of the brain showing compression of the ventricles; **(D, E)** gray matter, with expansion of the perivascular spaces highlighted by arrows (H&E, 200× and 400×); **(F)** perivascular fluid extravasated into the brain parenchyma (arrows) (H&E, 200×) with positive staining for **(G)** fibrin (phosphotungstic acid hematoxylin, 200×) and **(H)** IHC for factor VIIIA (200×); **(I)** positive perivascular immunofluorescence staining for fibrin (100×); **(J)** aberrant GLUT1 IHC staining in vascular endothelium (arrow) (400×); **(K)** white matter with myelin pallor and vacuoles (LFB-PAS, 400×) compared with normal (inset); **(L, M)** clasmatodendrosis with beading and fragmentation of the astrocytic processes in superficial cortex (GFAP IHC, 400× and 1000×); **(N)** perivascular distribution of damaged astrocytes within white matter (GFAP IHC, 200×); **(O)** infrequent scattered intraparenchymal inflammatory cells (LCA/CD45 IHC, 400×) with **(P)** rare T-cells (CD3 IHC, 400×); **(Q)** clusters of macrophages distributed around vessels (CD68 IHC, 400×); **(R)** activated rod-shaped microglia (arrow) (CD68 IHC, 400×).

The histologic findings were consistent with profound cerebral edema. There was widespread dilatation of the perivascular spaces (Fig. 1D, E) with the presence of an acellular eosinophilic substance (Fig. 1F) that stained for factor VIIIA (Fig. 1G) and fibrin (Fig. 1H, I), indicating perivascular fluid extravasation. IHC staining for GLUT1 showed aberrant staining in the endothelial cells in scattered vessels, suggesting endothelial damage (Fig. 1J). There was also vacuolization of the white matter tracts (LFB-PAS) (Fig. 1K), consistent with edema. Astrocyte injury was present throughout the superficial cortex and the white matter, with IHC highlighting aberrant beading and fragmentation of GFAP (Fig. 1L–N), a phenomenon termed clasmatodendrosis that is indicative of BBB dysfunction. The GFAP fragmentation was accentuated around the blood vessels (Fig. 1N). There was no evidence of cerebral thrombotic microangiopathy. Sections of the patient's cortex showed reduced endothelial expression of ICAM-1 and VCAM-1 compared with controls (Supplementary Data Fig. S1). Sections from control brains did not demonstrate clasmatodendrosis or perivascular fibrin extravasation.

We did not identify leukemia cells by flow cytometry performed on CSF (obtained at time of autopsy), which was paucicellular without a clearly defined lymphoid or blast population, or by histologic examination of the brain. We found scattered intraparenchymal CD45+ cells (Fig. 1O), including rare CD3+ T cells (Fig. 1P), aberrant perivascular CD68+ macrophages (Fig. 1Q), and activated rod-shaped microglial cells (Fig. 1R). We did not detect CAR T cells in the brain parenchyma with chimeric CD19 receptor CISH; appropriate signal was detected in control samples (Fig. 2).

There was no histologic evidence of CNS infection. In addition, bacterial and fungal cultures of CSF, PCR for human herpesvirus 6 and enterovirus on CSF, and adenovirus, cytomegalovirus, herpes simplex virus, and varicella zoster cultures of brain tissue were all negative. Examination of non-CNS organs revealed multiple hepatic fungal abscesses with hyphal forms with treatment-related degenerative changes (Supplementary Data Fig. S2A). Sections of lung showed mild pulmonary edema but were negative for diffuse alveolar damage. There was no evidence of systemic thrombotic microangiopathy or multiorgan failure. Flow cytometry performed on peripheral blood showed mostly nonspecific staining on poorly preserved cells without a clearly defined lymphoid or blast population. The bone marrow from a vertebral body, however, contained an increased number of CD20+ B cells (at least 30% of the marrow cellularity) with scattered admixed CD3+ T cells, consistent with ongoing involvement with B-cell ALL (Supplementary Data Fig. S2B–D).

## DISCUSSION

The overall findings in our examination of the brain from this patient are nonspecific and do not clearly point to one etiology or pathogenic mechanism for this case of cerebral edema following CAR T-cell infusion. However, the pertinent negatives of this case are important to consider. In particular, we did not identify an infectious process, and we did not identify intraparenchymal ALL cells, prominent infiltration of lymphocytes, or CAR T cells. The pertinent histologic findings of perivascular exudates with fibrin deposition, of activated microglia, and of fragmentation of GFAP termed clasmatodendrosis do not themselves support a particular mechanism of neurotoxicity but suggest a number of possibilities, including BBB disruption, astrocyte dysfunction, and high cytokine levels. Of note, these histologic changes are not attributed to postmortem changes, based on our institution's experience evaluating autopsy brains with a range of postmortem intervals, on reported histologic descriptions of variably decomposed brains (11) and on our examination of a comparable cohort of control brain specimens.

The presence of perivascular exudates with fibrin deposition raises the possibility that the CAR T-cell related neurotoxicity in this case may have resulted from endothelial and astrocyte injury with resulting BBB dysfunction. The decrease in fibrinogen and increase in D-dimer levels may suggest a role for concurrent disseminated intravascular coagulation. These findings are consistent with the features recently reported in a study of 53 patients with neurological adverse events seen after treatment by a different CD19 CAR T-cell product (5). Among those patients with severe neurotoxicity, there were elevated serum levels of endothelial proteins ANG2 and von Willebrand factor (VWF), which suggest increased endothelial cell activation and microvascular permeability. Moreover, high protein concentrations were present in the CSF, in keeping with BBB dysfunction. In addition, this series contained the postmortem examination of the brain from 2 patients with fatal neurotoxicity following CAR T-cell therapy, and histologic evidence of vascular disruption was present in both cases.

The absence of substantial lymphocytic infiltrates in our patient's brain suggests a central role for circulating serum cytokines in the adverse neurological effects of CAR T-cell therapy. The histologic findings in CAR T-cell related neurotoxicity overlap, in part, with those of posterior reversible encephalopathy syndrome (PRES) (12) and cerebral malaria in which high levels of circulating cytokines without overt lymphocyte accumulation have been implicated in BBB dysfunction and edema. The lack of interstitial edema in non-CNS tissues suggests selective vulnerability of the brain microvasculature. Cytokine activation of microglia may locally amplify the effects of cytokine dysregulation. Microglial activation is also observed in cerebral malaria, as is fibrinogen extravasation (13). Notably, our patient only had moderate CRS rather than the clinically severe CRS seen in other fatal cases. Thus, the relationship between CRS and the development of neurotoxicity requires further investigation.

Our analysis of cell adhesion molecule expression as a surrogate marker for elevated cytokines showed reduced levels of ICAM-1 and VCAM-1 in the endothelium of the patient's cortex. Although levels of adhesion molecules in BBB endothelial cells generally increase in response to cytokine exposure (14), the regulation of adhesion molecule expression is complex, with some cytokines inducing and others reducing their expression (15). Moreover, dexamethasone, which was administered several times to our patient to treat CRS and fulminant cerebral edema, has been shown to reduce adhesion molecule expression (16), therefore confounding our analysis of ICAM-1 and VCAM-1 endothelial expression.

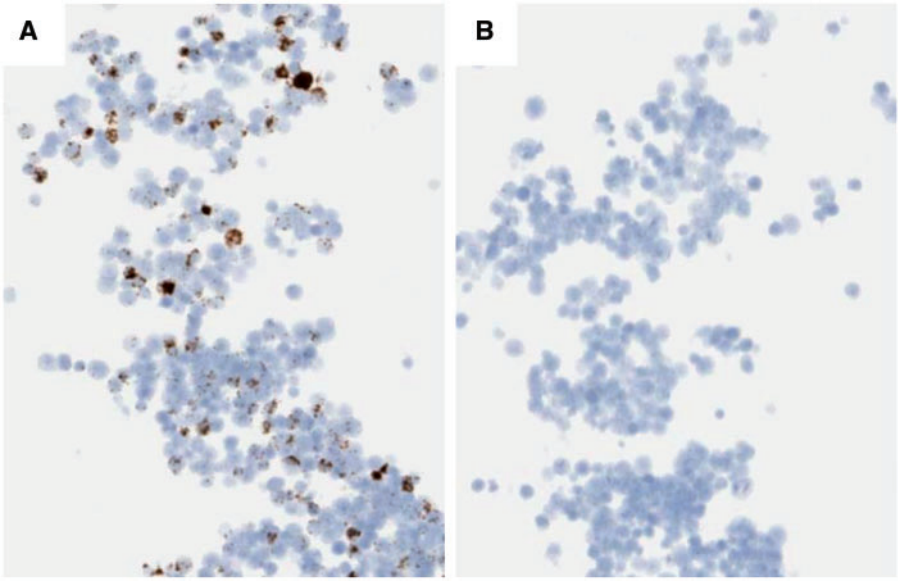


**FIGURE 2. (A)** Chromogenic in situ hybridization (CISH) directed against the chimeric CD19 receptor performed on cell pellets generated by spiking CAR T cells into healthy donor peripheral blood mononuclear cells revealed strong signal, indicating the presence of CAR T cells. No CAR T cells were detected in CNS tissue (image not shown); **(B)** CISH performed with a negative control probe showed absent staining.

The substantial amount of clasmatodendrosis in our case suggests that dysfunction of the astrocyte population may have contributed to the severe neurotoxicity seen. The etiology and implications of clasmatodendrosis, characterized by disintegration of the astrocytic processes and beading of GFAP, are not well-understood. It has been identified in a range of pathological states, including in brain trauma, ischemia, Alzheimer disease, multiple sclerosis, hyperglycemia and cerebral edema (17). In our case, clasmatodendrosis was also present in a perivascular pattern, potentially contributing to the dysfunction of the neurovascular unit of the BBB that is comprised of neurons, astrocytes, oligodendrocytes and microglia as well as the pericytes and endothelial cells of the blood vessels themselves. The effects of clasmatodendrosis seen in our case, however, likely extended beyond an impact on the BBB. GFAP beading was present throughout the cortex and white matter, not solely in a perivascular pattern, suggesting a more general neuropathologic effect.

While high-dose fludarabine led to necrotizing leukoencephalopathy when first tested in clinical trials (18), the lower doses that are now currently used for lymphodepletion prior to CAR T infusion are generally well-tolerated. Used to facilitate expansion of CAR T cells (7), lymphodepletion with fludarabine and other agents can be associated with the development of severe CRS, thus playing an indirect role in neurotoxicity. Whether there is a direct impact of fludarabine or elements of the CAR T-cell manufacturing/expansion process on the adverse neurological events in patients treated in this CAR T-cell trial remains unclear. In the CD19 CAR T-cell trial in which our patient was participating (NCT02535364), multiple cases of cerebral edema were temporally correlated with addition of fludarabine to the lymphodepletion regimen previously consisting of cyclophosphamide alone. However, many clinical trials use fludarabine and cyclophosphamide-based lymphodepleting regimens with no or very infrequent cases of subsequent cerebral edema (2–4), suggesting that this preconditioning combination is not in itself problematic. Thus, the distinct role of fludarabine in this patient or in other patients with fatal neurologic adverse events is uncertain.

This report adds to the important study by Gust et al (5). It strengthens the association between potential BBB dysfunction and severe neurotoxicity in patients treated with CAR T cells. We provide additional characterization of the neuropathologic changes seen with CAR T-cell-associated fatal edema, including the presence of clasmatodendrosis. In contrast to the neuropathologic description of 2 patients with severe neurotoxicity included by Gust and colleagues, evaluation of this patient's CNS tissue did not show intraparenchymal hemorrhages, infarcts, fibrinoid vessel wall necrosis, intravascular platelet microthrombi, or infiltration by CAR T cells, highlighting the spectrum of changes that can be observed particularly between different CAR T-cell products and trials.

Our study is limited by several factors. First, we do not have data on the cytokine levels in the peripheral blood or CSF in our patient and therefore cannot correlate these levels with the patient's neurotoxicity. Second, the observed histologic changes are compatible with but not diagnostic of BBB dysfunction. Furthermore, we have not identified the underlying mechanism of the potential BBB dysfunction.

Experimental models that recapitulate CRS and neurotoxicity are needed to explore and elucidate mechanistic aspects of the neurological adverse events that occur during CAR T-cell therapy. A robust system for clinical monitoring of adverse effects partnered with a rapid, coherent response system and avenues for disseminating information will be of great value to the immunotherapy field and to the wider

discipline of regulatory science. Despite significant setbacks, CAR T cells remain highly promising anticancer immunotherapeutics. The presented data highlight a striking but infrequent adverse effect of CAR T-cell therapy—profound and fatal cerebral edema—and offer some insight into the potential pathophysiology of a devastating complication, namely BBB dysfunction, whose mechanism demands further elucidation.

## ACKNOWLEDGMENTS

*We thank Dr. Rebecca Folkerth and Dr. Helmut Renke for very helpful discussions. We thank Terri Woo for assistance with staining.*

## REFERENCES

1. Maude SL, Frey N, Shaw PA, et al. Chimeric antigen receptor T cells for sustained remissions in leukemia. N Engl J Med 2014;371:1507–17
2. Neelapu SS, Locke FL, Bartlett NL, et al. Axicabtagene ciloleucel CAR T-cell therapy in refractory large B-cell lymphoma. N Engl J Med 2017; 377:2531–44
3. Schuster SJ, Svoboda J, Chong EA, et al. Chimeric antigen receptor T cells in refractory B-cell lymphomas. N Engl J Med 2017;377:2545–54
4. Turtle CJ, Hay KA, Hanafi LA, et al. Durable molecular remissions in chronic lymphocytic leukemia treated with CD19-specific chimeric antigen receptor-modified T cells after failure of ibrutinib. J Clin Oncol 2017;35:3010–20
5. Gust J, Hay KA, Hanafi LA, et al. Endothelial activation and blood-brain barrier disruption in neurotoxicity after adoptive immunotherapy with CD19 CAR-T cells. Cancer Discov 2017;7:1404–19
6. Lee DW, Gardner R, Porter DL, et al. Current concepts in the diagnosis and management of cytokine release syndrome. Blood 2014;124: 188–95
7. Turtle CJ, Hanafi LA, Berger C, et al. CD19 CAR-T cells of defined CD4+: CD8+ composition in adult B cell ALL patients. J Clin Invest 2016;126:2123–38
8. DeAngelo DJ, Ghobadi A, Park JH, et al. Clinical outcomes for the phase 2, single-arm, multicenter trial of JCAR015 in adult B-ALL (ROCKET Study). Society for Immunotherapy in Cancer (SITC). Abstract #217. 2017.
9. Larsen EC, Devidas M, Chen S, et al. Dexamethasone and high-dose methotrexate improve outcome for children and young adults with high-risk B-acute lymphoblastic leukemia: A report from Children's Oncology Group Study AALL0232. J Clin Oncol 2016;34:2380–8
10. Lew G, Lu X, Yanofsky R, et al. Outcomes after intermediate-risk relapse of childhood B-lymphoblastic leukemia (B-ALL) and the role of allogeneic stem cell transplantation (SCT): A report from Children's Oncology Group (COG) AALL0433. Blood 2014;124:684
11. MacKenzie JM. Examining the decomposed brain. Am J Forensic Med Pathol 2014;35:265–70
12. Kheir JN, Lawlor MW, Ahn ES, et al. Neuropathology of a fatal case of posterior reversible encephalopathy syndrome. Pediatr Dev Pathol 2010; 13:397–403
13. Dorovini-Zis K, Schmidt K, Huynh H, et al. The neuropathology of fatal cerebral malaria in malawian children. Am J Pathol 2011;178:2146–58
14. Varatharaj A, Galea I. The blood-brain barrier in systemic inflammation. Brain Behav Immun 2017;60:1–12
15. Hosokawa Y, Hosokawa I, Ozaki K, et al. Cytokines differentially regulate ICAM-1 and VCAM-1 expression on human gingival fibroblasts. Clin Exp Immunol 2006;144:494–502
16. Yang JT, Lee TH, Lee IN, et al. Dexamethasone inhibits ICAM-1 and MMP-9 expression and reduces brain edema in intracerebral hemorrhagic rats. Acta Neurochir (Wien) 2011;153:2197–203
17. Sakai K, Fukuda T, Iwadate K. Beading of the astrocytic processes (clasmatodendrosis) following head trauma is associated with protein degradation pathways. Brain Inj 2013;27:1692–7
18. Spriggs DR, Stopa E, Mayer RJ, et al. Fludarabine phosphate (NSC 312878) infusions for the treatment of acute leukemia: Phase I and neuropathological study. Cancer Res 1986;46:5953–8